Experimental Thermal and Fluid Science 35 (2011) 1463–1472

Contents lists available at ScienceDirect

Experimental Thermal and Fluid Science

journal homepage: www.elsevier.com/locate/etfs

Experimental study on thermal uniformity of optical transmitter and receiver on near space

Yao Lei [a,*], Zhijun Xu [a], Lizhong Zhang [b]

[a] Changchun Institute of Optics, Fine Mechanics and Physics, Chinese Academy of Sciences, Graduate School of Chinese Academy of Sciences, Changchun, Jilin Province, China
[b] Institute of Space Optoelectronic Technology, Changchun University of Science and Technology, Changchun, Jilin Province, China

ARTICLE INFO

Article history:
Received 31 March 2011
Received in revised form 19 May 2011
Accepted 16 June 2011
Available online 24 June 2011

Keywords:
Thermal uniformity
Near space
Cladding
Optical transmitter and receiver

ABSTRACT

According to the special airframe construction of the prototype and the particular environment of the near space, the thermodynamics modeling simulation is designed to instruct the temperature-rise tests on the ground and guarantee the steady operation of the optics, electronics and mechanical structure system in optical transmitter and receiver, which demonstrated the goodness of fit for theoretical and experimental analysis. In the meantime, the temperature-rise tests for the critical components and physical model are controlled by BP algorithm which saved experimental periods and improved the conventional efficient. In the end, the internal temperature field distribution in the optical transmitter and receiver is analyzed in this paper, and how to keep the uniformity of the thermal field in a short time is studied as well. And the analytic results show that the experiments satisfy the required indices, what's more, the analytic process may supervise the analytical calculation of the same type optical transmitter and receiver, which is worth using in engineering.

1. Introduction

With the development of the new type optical transmitter and receiver applied on the near space, the investigation of the thermal uniformity and their applications in to demonstrate the environmental flexibility are studied recent years. Numerous theoretical studies of suspensions containing environmental effects on the aircrafts have been conducted initiating studied on the near space. However, due to the special characteristics of the near space and the special structure of the optical transmitter and receiver, it is a challenge to study on the thermal uniformity of the whole airframe. The lack of stability of such suspensions induced additional experimental study on thermal uniformity.

A considerable experimental and theoretical works have been done on the application and design modification for improving the thermal performance. Recent works have shown that the presence of the cladding measures in thermal experiments causes an important enhancement of his thermal characteristics [1]. In the present study, physical model is employed as working medium for the prototype to investigate the thermal performances of the optical transmitter and receiver [5]. Thus, the different experiment schemes are considered. The results are finally compared with the thermal performance of the different working modes.

The key function of the temperature control measures is supplying an isoperibol for the optical transmitter and receiver, and simulating the environment characteristics of the near space to study the internal temperature uniformity. How to realize the uniformity analyses of the thermal field through the thermal analysis with the finite space and the finitude power are the emphasis in this paper.

1.1. Environmental characteristics

The near space is the airspace usually defined as 10 km to 100 km, which is between the maximum flight altitude of the airplane and the minimum orbital height of the satellite, and approximately including stratosphere, mesosphere and part of ionosphere [1]. It is very important to study the internal temperature field distribution of the optical transmitter and receiver to guarantee the optics and electronics system working stable at the prescribed limit [2]. Compared with other environmental factors like humidity, pollution, erosion, abrasion, efflorescence and radiation, the temperature, as the most important technical parameter, has been taken into consideration during the thermal uniformity [12]. Most of the near space lied in the stratosphere, the temperature is higher in the upside while it is lower in the downside, the atmosphere convection is weak, and the temperature environment is relatively low, probably is −50 °C and the atmosphere density is small. So we focus on the typical environmental characteristic of the 20 km, the wind direction and the temperature is relatively stable, and the characteristics are as followed.

* Corresponding author.
E-mail addresses: ly030312101@126.com (Y. Lei), xuzj538@ciomp.ac.cn (Z. Xu), zlzcust@126.com (L. Zhang).

0894-1777/$ - see front matter © 2011 Elsevier Inc. All rights reserved.
doi:10.1016/j.expthermflusci.2011.06.005

Nomenclature

α_g	expansion coefficient of glass (10^{-6}/K)
n_g	refractive index of glass
η_a	refractive index of air
P	air pressure (MP)
P_0	normal atmosphere (MP)
ΔT	temperature variable (K)
M_0	moment of friction which is irrelevant to the load (N·mm)
D_m	mean diameter of bearing (mm)
f_0	lubrication factor, grease lubrication of the angular contact ball bearing, When the bearing is unistrand $f_0 = 2$
n	bearing rotation speed (r/min)
v_0	dynamic viscosity of the lubricant at the working temperature (mm^2/s)
f_1	correlation factor
N_1	bearing load (N)
N_0	equivalent static load (N)
C_0	basic normal static load (N)
X_0	static radial coefficient is 0.5 when the unistrand nominal angle of the annular ball bearing is 25°
Y_0	static axial coefficient is 0.5 when the unistrand nominal angle of the annular ball bearing is 25°
F_r	radial load (N)
F_a	axial load (N)
H_f	the thermal value of the shafting (W)
M	friction moment (N·mm)

Distribution of the temperature and pressure [3]:

$$\text{Temperature}: T_{a0} = 216.65 \tag{1}$$

$$\text{Pressure}: p_{a0} = 22631.8 \exp\left[\frac{11000.0 - v}{6340}\right] \tag{2}$$

$$\text{Density}: \rho_{a0} = 0.3639 \exp\left[\frac{11000.0 - v}{6340}\right] \tag{3}$$

Variation of the wind field:

Considering the stratosphere latitude range of China, the vertical convection is not strong, and the advection is more often, the wind is even, east wind is popular in summer, and the wind speed is small, generally is 5 m/s to 10 m/s; the west wind is more often in winter, and the wind speed is relatively large, generally is 15 m/s to 25 m/s [6].

1.2. Investigated subject

The optical transmitter and receiver we studied mainly include a spherical turret with photoelectric equipment whose diameter is φ380 mm, and an electronic box for controlling. The basic structure of the prototype is showed in Fig. 1.

Inside the spherical shell, the shock absorber is jointed with the inner frame, and the outer pitch axis outside the spherical shell is attached with the outer frame. The protective casing is fixed fore and after, which is formed a seal cavity structure. The gimbal mount inside the spherical shell contains two DOF of azimuth and pitching, which largely include angular transducer, measurement unit, gyro, drive motor. The whole airframe is compounded by two shafting structures, pitch axis and azimuth axis. The optical section, laser transmission and receiving system are mounted on the inner frame, and the protective casing is designed to be dustproof and pressure adjustable [5].

Fig. 1. Prototype of the optical transmitter and receiver with φ600 mm.

The effects of the ambient temperature fluctuation on the optical instruments in the optical transmitter and receiver are as followed:

(1) Characteristic parameters of the optical components will change with the temperature fluctuation, which lead to the descent of the picture elements. Taken the optical glass for example, thermal deformation of the thickness and outside diameter may cause the variance of the dispersion and refractive index which eventually result in the change of the focal length. The relation between the temperature fluctuation and the focal length of plotting lens is represented as followed.

$$\Delta f = \left[\alpha_g + \frac{n_g P}{(n_g - 1)P_0}\eta_a - \frac{\eta_g}{\eta_g - 1}\right] f \Delta T \tag{4}$$

(2) Thermal gradient is formed in the whole inner frame, and the additional heat stress and loading force are overlapped when there is a large temperature gradient, and this may affect the carrying capacity [4].

(3) Thermal transient (thermal shock) is another problem resulted by the ambient temperature fluctuation. For the camera inside the machine, when there is a temperature step about 12 °C, the defocus is −0.23 mm, and the resolution drop down from 100 line pair per millimeter to 20 line pair per millimeter, which need 5–6 h to be stable [12].

Above all, in order to insure the key parts of the optical transmitter and receiver to work safely and stable in the near space, the thermal uniformity research is necessary.

1.3. Thermal resource analyses

After the comprehensive consideration on the mechanical structures of the optical transmitter and receiver, we mainly focus on the inner frame where the most thermal resources are centered, such as the azimuth and the pitching motors. The pitch shafting of the electromotor is selected to be the representative subject, and the structure is showed in Fig. 2.

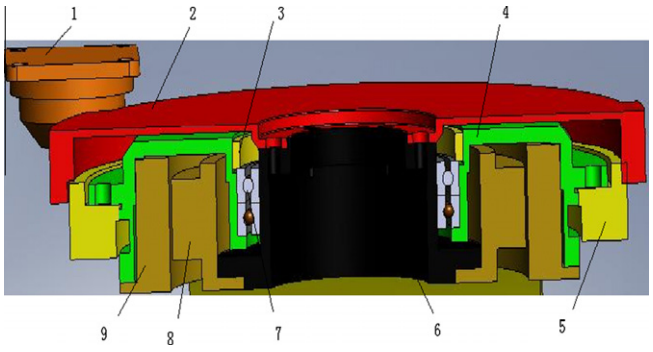

Fig. 2. Shafting structure. (1) shock absorber (2) motor enclosure (3) end ring (4) outer shaft of the motor (5) inner frame (6) inner spindle of the motor (7) bearing (8) electric machine rotor (9) electric machine stator.

The shafting is driven by the motor which is the mainly thermal resource, and the frictional heat of the bearings is not negligible. Motors inside the optical transmitter and receiver are straight-drive with low speed, so the rotation speed is 200 r/min to 500 r/min and we can get the friction thermal value of the shafting from computing [11].

To stabilize the temperature range, the frame model is simplified, and just the main heat resources are considered to compute the heat power: the grand totals of the rolling friction, the liding friction and the lubricant friction generated by bearings may bring the drag friction moment, which generally include two parts, M_0 and M_1 [6].

$$M = M_0 + M_1 \tag{5}$$

(1) Compute M_0 which is irrelevant to the bearings:
When $v_0 n \geqslant 2000$:

$$M_0 = 10^{-7} f_0 (v_0 n)^{2/3} D_m^3 \tag{6}$$

When $v_0 n < 2000$:

$$M_0 = 160 \times 10^{-7} f_0 D_m^3 \tag{7}$$

(2) Compute M_1 which is relevant to the bearing load and include the friction loss caused by the differential action of the elastic lag and faying surface:

$$M_1 = f_1 N_1 D_m \tag{8}$$

Bearing load of the angular contact ball bearing:

$$N_1 = 0.0013 (N_0 / C_0)^{0.33} \tag{9}$$

Computing formula of N_0 [6]:

$$N_0 = X_0 F_r + Y_0 F_a \tag{10}$$

where $N_0 = F_r$, when $N_0 < F_r$.
Then the thermal value caused by the friction moment is:

$$H_f = 1.047 \times 10^{-4}\ \text{nM} \tag{11}$$

When the pitching motor speed is 500 r/min, the internal heat sources of the optical transmitter and receiver which are mostly generated by motor shafting whose thermal value is 5.2 W, the azimuth shafting whose thermal value is 5 W, the swing angle sensor whose maximal power is 10 W, the CCD camera whose power is 2.2 W according to the technical parameter, the laser in optical platform whose power is 10 W, and the motors at the inner frame whose power is 20 W under the normal operating conditions. And the whole heat formed the circulation flow inside the frame.

2. Experiments

2.1. Experimental setup

To satisfy the requirement of the flight-test, the whole experiment is divided into two parts: cladding experiments to demonstrate the thermal field theory with active (heating with electricity) and passive (heat preservation) temperature control measures, and the temperature-rise tests to get the holding time for 4000 m flight test.

Cladding experiment scheme: First of all, ascertain the power range when the temperature is stabilized 10 °C to 20 °C without cladding, then compute the layer of the heat insulating material, ascertained the power range and the thermal insulation effect, at last, leave one face without cladding to simulate the optical window to ascertain the thermal insulation effect.

Temperature-rise test scheme: To gain the required time and the power range from −40 °C to 0 °C (most materiel devices can work normally at 0 °C), different test modes will be considered, which include the cladding mode and the isolated layer mode with different heating power to compare the thermal performance when the optical transmitter and receiver can resume to the work mode.

Considering the thermal inertia effect, there is a deflection between the experimental temperature and the thermal balance temperature, and according to the GJB1033A of "heat balance test method for spacecraft" in China, the prescriptions are as followed [7]:

(1) When the working condition is the steady state, the temperature fluctuation of the experimental monitoring point is not more than ±0.5 with 4 continuous hours;
(2) When the working condition is the transient state, the temperature fluctuation is no less than 1 °C in the four test periods.

For the stability test, the temperature fluctuation velocity is very small when the experiment finished, and the internal energy variation is negligible compared with the internal heat source, or there is a major error between the experimental result and the true value. When the inner temperature reach the test temperature range, the temperature holding time is needed to make the interior assembly achieve the thermal balance temperature. And the holding time is decided by the different subassembly with different quality [8]. According to the experiment regularity, the temperature holding time is showed in Table 1.

Above all, when the environmental characteristics of 20 km in near space is studied well, the initial heat source of the heating elements in the inner frame is completely computed, and the whole cladding and isolated layer experimental schemes are designed, a series of thermal balance tests will be performed in order to satisfy the working index as followed:

(1) The given ambient temperature −50 °C to 0 °C;
(2) The temperature in the inner frame is requested to stabilize at 20 ± 2 °C;
(3) The experimental power consumption is less than 1000 W.

Table 1
Temperature holding time for different subassembly with different quality.

Quality (kg)	Holding time (h)
⩽2	⩾0.5
>2–8	⩾1
>8–15	⩾1.5

2.2. Experimental fields

The variation of the experimental conditions allow for monitoring the inner temperature and the heating power. For preparation of the physical model used in this work, the isolated box and the optical window were optimized and fixed as followed in Fig. 3.

Local temperature in the box was measured by a thermo-couple with the type P-100 thermo-resistance [10]. The uncertainty in temperature measurements was ±0.1 °C. And the thermo-resistance was mounted on the mount section.

The resistive heater mounted in the model was simulated as the inner heat resource of the optical transmitter and receiver, and the temperature of the practical object was monitored. The caliber with 120 mm of the cylinder was simulated as the optical window to test the impact of the optical window on the whole temperature control measures [9].

The pro rata practical temperature model was adopted in the experiment to simulate the optical transmitter and receiver in the near space. The ambient temperature of the near space was simulated by the high-low temperature test chamber, the pressure variation was simulated by the pump and vacuum container, and the temperature measurement was achieved by the temperature probe. The system used for thermal performance measurement of the pro rata practical model is shown in Fig. 4.

Fig. 3. Pro rata model.

Fig. 4. Experiment field. (a) Multilayer parcel in the low-pressure pot. (b) Airproof disposal and high-low temperature test chamber.

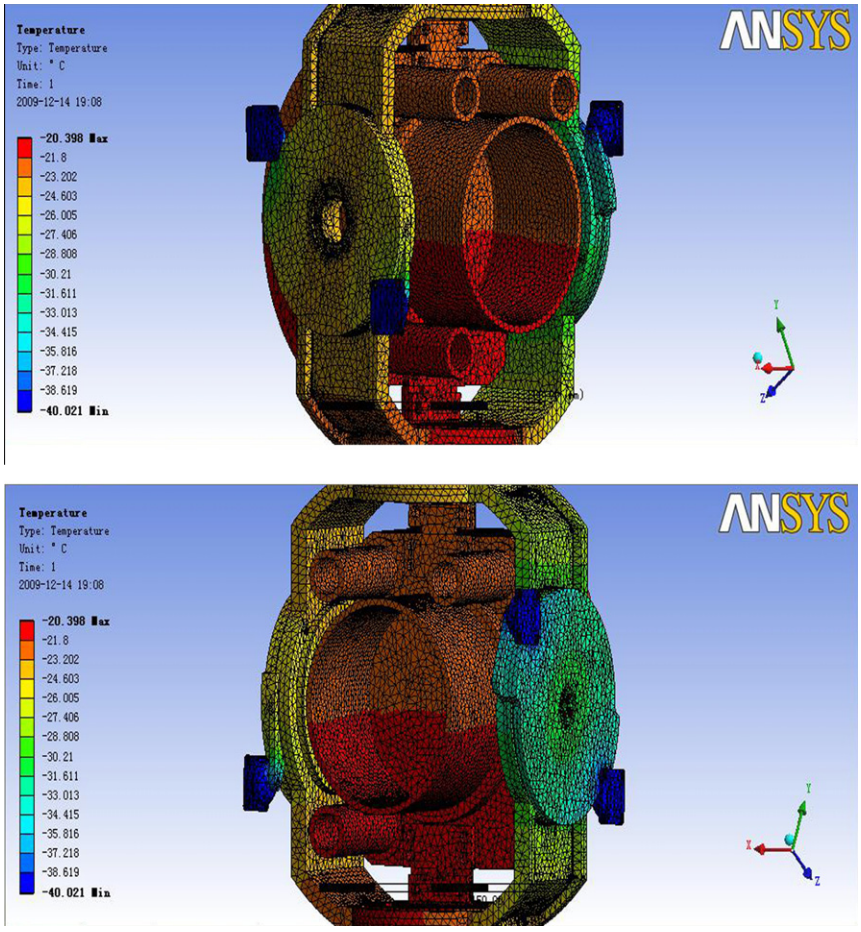

Fig. 5. Simulation result.

Table 2
Cladding tests data.

No.	Ambient temperature (°C)	Heating power (W)	Inner temperature (°C)	Pressure (Mpa)	Cladding state	Relative height (m)
1	−50	40	−12.6	0.1	10 layers	0
2	−55	40	−16.9	0.1	10 layers	0
3	−55	54	13.4	0.1	20 layers	0
4	−55	31	21	0.013	20 layers	14,500
5	−55	28.5	16.2	0.013	20 layers	14,500
6	−55	30.4	19.7	0.01	20 layers	16,000
7	−55	28	13.9	0.014	20 layers	14,000
8	−55	30.4	14.6	0.024	20 layers	10,600
9	−55	30.4	13.3	0.026	20 layers	10,000
10	−55	27.5	7.9	0.026	20 layers	10,000
11	−55	27.6	3.7	0.046	20 layers	6200
12	−55	30.4	7.2	0.046	20 layers	6200
13	−55	28.5	13.1	0.016	20 layers with optical window	13,000
14	−55	29.9	14.4	0.016	20 layers with optical window	13,000
15	−55	28	7.3	0.03	20 layers with optical window	9200
16	−55	31.5	13.1	0.03	20 layers with optical window	9200
17	−55	35.8	19.5	0.03	20 layers with optical window	9200
18	−55	33.8	17.8	0.03	20 layers with optical window	9200
19	−55	33.8	15.1	0.04	20 layers with optical window	7200
20	−55	33.8	13.4	0.05	20 layers with optical window	5600
21	−55	31.5	8.1	0.062	20 layers with optical window	4000
22	−55	35.6	13.6	0.062	20 layers with optical window	4000
23	−55	42.7	25.2	0.062	20 layers with optical window	4000
24	−20	60.3	37.8	0.062	No cladding	4000
25	−20	38.3	20.2	0.062	No cladding	4000
26	−20	30.7	13.4	0.062	No cladding	4000
27	−10	60.5	47	0.062	No cladding	4000
28	−10	30.1	22.5	0.062	No cladding	4000
29	−10	27.6	14.9	0.062	No cladding	4000
30	0	21.6	24.7	0.062	No cladding	4000
31	0	12	15.3	0.061	No cladding	4000

2.3. Bp algorithm for heating time

Temperature control time is long and the control efficiency is low during the experiment while the temperature control impacted by 4 factors. To stabilize the inner temperature, the BP network is simple and fast when there are multivariable inputs. Ensure the inner temperature stabilize at the required range is the ultimate control objective in the temperature feedback regulative stabilization system.

The temperature of optical transmitter and receiver was predicted through the BP algorithm based on MATLAB simulation platform. The given inner temperature was affected by ambient temperature, heating power, air pressure, cladding mode, whose stabilization needed corresponding adjustment of these conditions. And the BP network structure with 4–8–5–1 was adopted, the Tansig function was applied in the implication layer, at the same time, the Purelin function was applied in the output layer. At last, the finite samples were trained and tested through the Matlab [5].

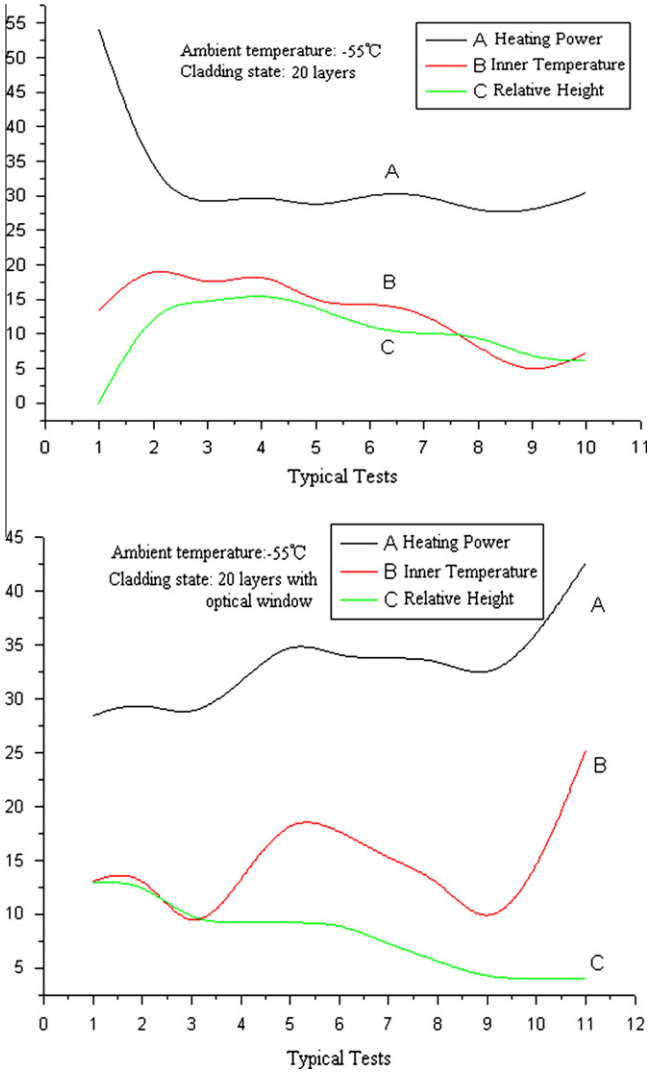

Fig. 6. Variation curve of the heating power and internal temperature at the different altitude when the ambient temperature is −55 °C.

3. Simulation and contrast

The temperature contour and heat flux after the loading and computing the boundary condition is showed in Fig. 5.

According to the simulation results, when the external temperature is −40 °C, friction thermal value of the shafting is 5.2 W, and the thermal value of the motor is 40 W. The maximum tempera-

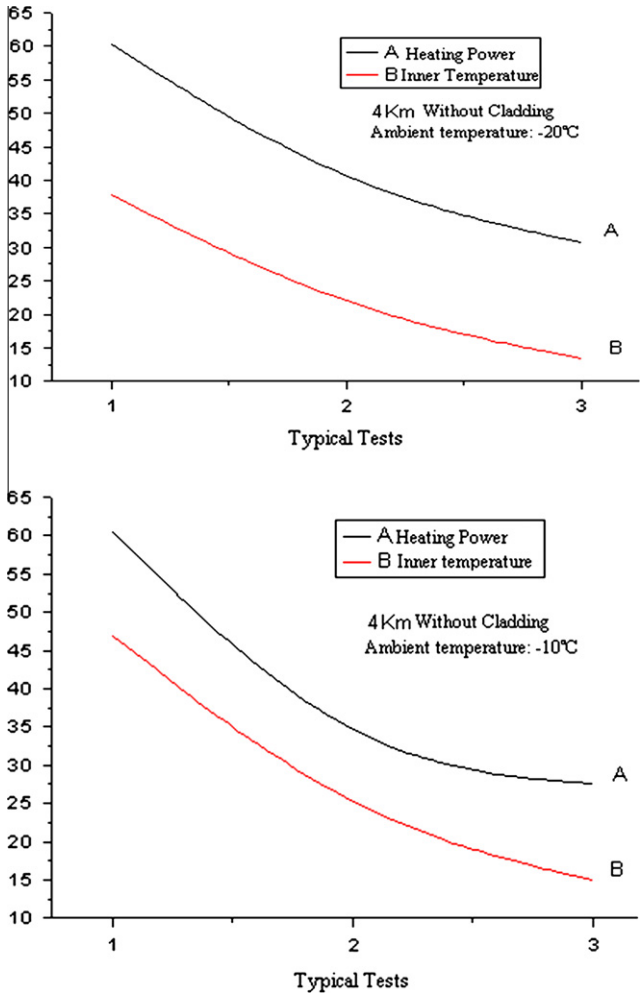

Fig. 7. Variation curves of heating power and inner temperature.

Table 3
Experiments without cladding on the height of 4000 m.

Ambient temperature (°C)	Heating power (W)	Inner temperature (°C)	Air pressure (Mpa)	Cladding state	Relative altitude(m)
−20	60.3	37.8	0.062	No cladding	4000
−20	38.3	20.2	0.062	No cladding	4000
−20	30.7	13.4	0.062	No cladding	4000
−10	60.5	47	0.062	No cladding	4000
−10	30.1	22.5	0.062	No cladding	4000
−10	27.6	14.9	0.062	No cladding	4000

ture is presented at the shafting, and the temperature of the optical platform connected with motor shafting is also high. Because of the big area of dissipation, the temperature of both sides is gradual decrease from the center, and the temperature of the bearings on both sides is nearly −20 °C, and the lowest temperature is on the spherical shell.

4. Results and discussion

4.1. Data analysis for cladding experiments

The cladding tests data is showed in Table 2.

In Table 2, it is clearly that there are only 3.5 W from the 27.5 W to 31 W between 10 km and 14.5 km in near space, when the ambient temperature is −55 °C and the cladding state is 20 layers, and the inner temperature fluctuation is 2 °C at the same altitude, which means the thermal deformation of the structural member in the inner frame is very small, and the effect on the optical components is weak. In addition, considering the heating time is stable, the deformation and the thermal gradient can be resumed during the heating time quickly. So the environmental flexibility and the thermal uniformity of the optical transmitter and receiver are pretty good at this phase.

According to the data, when the maximal heating power is 60 W, it is capable to maintain the required temperature range, which saved the heating power, and we can consider more functions for other units during the miniaturization. The curves are formed by cladding mode, ambient temperature, heating power, internal temperature, and relative height and showed in Fig. 6.

From Fig. 6, we know that the variation trend of the heating power is similar with the internal temperature while the relative height is various. When we consider the optical window at the 20 layers cladding mode, the internal temperature is similar with the condition without the window, so the thermal insulation effect is the same whether we considering the optical window, which means that the window hardly impact the whole thermal insulation effect.

4.2. Data analysis for the temperature rise tests

To prepare the patrol flight-test on the height of 4000 m, the test was repeated with varying parameters such as ambient temperature, heating power and air pressure.

According to the table of standard atmosphere, we know that the temperature of 4000 m is −11 °C, to simulate the cold side mode of the airframe in the lift process, a series of tests at −20 °C were done for contrastive analysis. The data without cladding on the height of 4000 m is presented in Table 3. And the variation trend is showed in Fig. 7.

From the figures above, we can see that the variation trend is conform with the whole thermal insulation effect trend, and only 30 W is needed to maintain around 13 °C, the cladding thermal insulation effect is perfect, easy to operate and credible, even when the special weather condition come up, the thermal insulation effect is still good.

The temperature-rise test from deep cooling −40 °C to 0 °C is performed to ascertain the minimum duration to make the optical

Table 4
Heating time table when the power is 60 W with 20 layers cladding.

Interval (min)	Inner temperature (°C)	Remark
0	−40	Start heating
12	−31.3	
11	−17.9	
10	−8.8	
11	−1.4	
3	0.0	Stop heating
2	0.2	
1	0.1	
0.5	0.0	
0.5	−0.1	

Table 5
Heat power is 110 W without cladding.

Interval (min)	Inner temperature (°C)	Remark
0	−40	Start heating
26	−19.8	
11	−18.9	
24	−18.4	
1	−18.5	
7	−18.4	
5	−18.4	
3	−18.4	

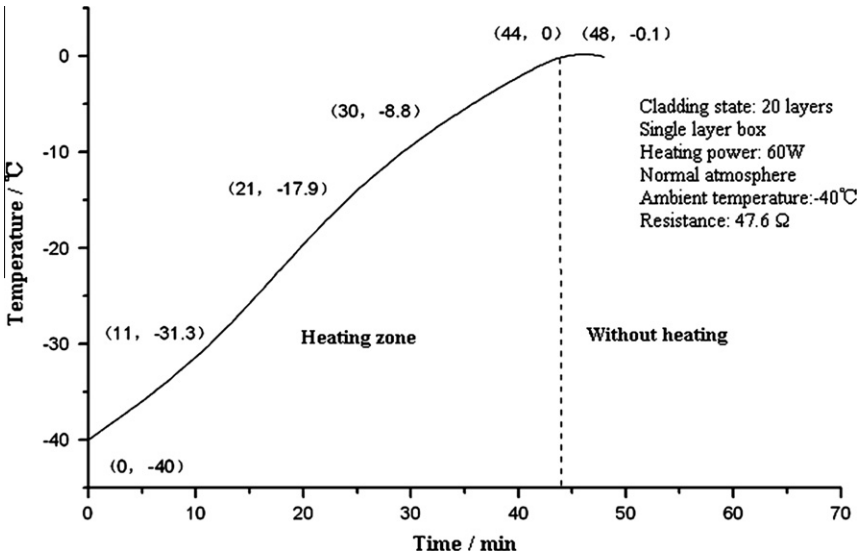

Fig. 8. The temperature rise curve when the heating power is 60 W with 20 layers cladding.

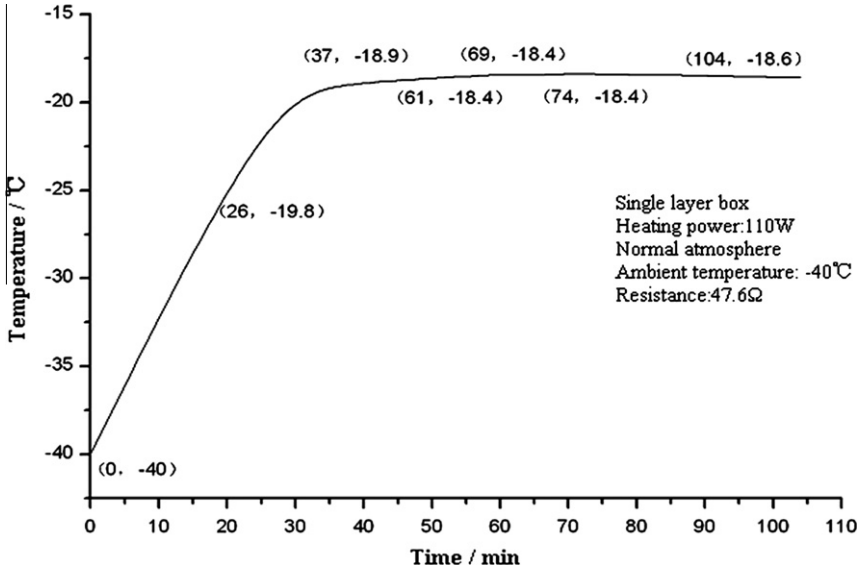

Fig. 9. Temperature rise curve when the heating power is 110 W without cladding.

transmitter and receiver start to work as soon as possible. It is meaningful to get work in a short time for the patrol flight-tests which may save the power and advance the work efficiency.

To contrast the power consumption, the temperature rise tests with 20 layers cladding are carried out at the normal pressure. The maximum power in Table 2 is 60 W, and the maximum power we assumed is 110 W, and there are only 28 min to get at 0 °C and the data of temperature rise characteristic with 60 W is presented in Table 4.

From the table, we can see that when the heating power is 60 W, the time for the temperature rise is 44 min, the temperature fluctuation is slow and the duration is relatively long and we can conjecture the thermal inertia from the curve from Fig. 8.

When the maximum power without cladding is 110 W and the temperature rise data are as followed in Table 5.

When the heat power is 110 W without cladding, the inner temperature can only maintain at −18.4 °C, which does not satisfy the requirement, and the temperature rise curve showed in Fig. 9.

In consideration of the high altitude environment of 4000 m, which is not severe as space environment, the nested mock-up for isolated layer test is adopted to compare with the cladding experiments, and when the heating power is 60 W, the data is showed in Table 6. From the table, we know that the time to warm up is just 14 min in nested isolated layer experiment without cladding. And the corresponding characters are showed in the Fig. 10.

Table 6
Temperature-rise test data with nested isolated layer.

Internal (min)	Inner temperature (°C)	Remark
0	−39.6	Start heating
9	−12.4	
1	−9	
2	−2.3	
1	0.0	
1	1.0	Stop heating
3	−1.0	
7	−5.5	
5	−10.4	
5	−17.9	

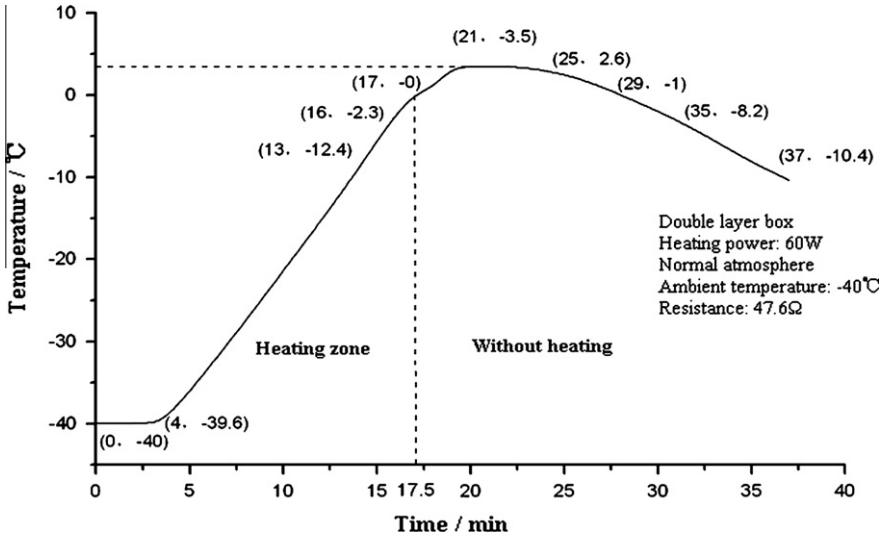

Fig. 10. Temperature rise curve when the heating power is 60 W with isolated layer.

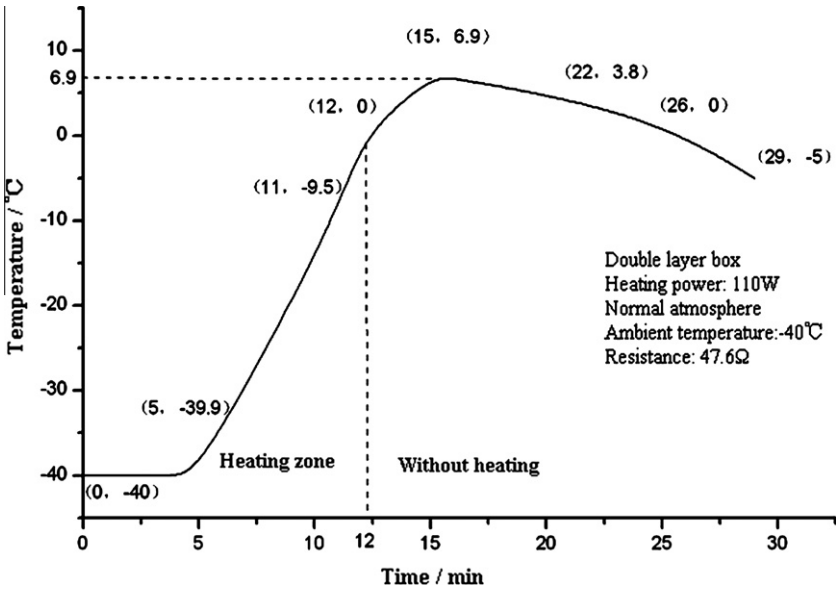

Fig. 11. Temperature rise curve when the heating power is 110 W with isolated layer.

Compared with the 60 W with cladding, we can save nearly half an hour which is useful for the optical transmitter and receiver to work efficiently.

And when the heating power is 110 W, the temperature rise more quickly, there is only 7 min. The curve is showed in Fig. 11. For the patrol flight-test on the height of 4000 m, the effect of the nested mock-up is obvious, and it also may supply more reference about the multi-temperature control of thermal uniformity for the optical transmitter and receiver.

Above all, the heat time and the heating power may be saved by reducing the heating volume when the power range is given. Owing to the air buffer formed by the interior air flow, the effect is good as the cladding with multilayer heat insulating material. And considering the practical operability, the isolated layer measure will be adopted in the thermal insulation of 4000 m.

5. Conclusions

Experimental investigation was carried out on the effect of various parameters on the thermal performance of the optical transmitter and receiver, using pro rata model as the experimental subject, focusing on the environmental characteristics of 20 km in near space, different heating power, air pressure and ambient temperature were considered in the cladding experiments and temperature-rise tests for 4000 m patrol flight, cladding measures were experimentally examined and results were compared with the isolated measures. To compare the thermal effect of the optical window, more tests to simulate the optical window were performed.

The experimental results clearly present the effect of ambient environment on the optical transmitter and receiver. The results of this study demonstrated that with each concentration levels of thermal tests, the performance was different.

Based on the analysis of the experimental investigations presented in this paper, the conclusions are as follows:

(1) The thermal performance of the optical transmitter and receiver is influenced by ambient temperature, air pressure, cladding mode and heating time due to presence of the special environmental characteristics in the theoretical analysis. And the ambient temperature is simulated with the high-low temperature test chamber, the air pressure is adjusted with the pump, the cladding mode is divided into 3 modes, and the nested mock-up is compared with the cladding state in the experimental analysis.

(2) The cladding tests with different parameters were performed and the thermal performance expressed by the performance curves. The needed maximal heating power was 60 W and it was enough to maintain 10 °C to 25 °C for the whole airframe which saved power for other units during the miniaturization. The heat dissipating capacity of the optical window is small and negligible.

(3) The maximal heating power of the temperature-rise tests for 4000 m patrol flight is assumed as 110 W, when the isolated measure was applied, which is not only reducing the heating space, but also saving the heating power. In addition, the thermal performance is good as the cladding measures. Considered the difficulties of the cladding for the joint of the moving parts, and the time limits for the temperature rise, the isolated layer measure is adopted for the CCD cameras in the airframe.

(4) The simulation tests with Matlab based on the experimental data have been done to predict the inner temperature, the results have presented that the generalization ability of the BP network can direct the practical temperature control experiments in the next period while the required accuracy in this paper is relatively low. Through the ANSYS simulation, the results are accordant with the test results, which demonstrate the feasibility for this temperature control system.

Acknowledgements

We would like to thank the Changchun Institute of Space Optic-Electric Technology for offering the experimental field.

References

[1] Guangwu Zhu, Baoquan Li, Space environment effect and countermeasure research on spacecraft, Journal of Aerospace Shanghai 45 (3) (2002) 1–7.

[2] Yajuan Liu, Research on space distribution scheme of near space positioning platform station, Journal of Radio Engineering of China 109 (2008) 5–8.
[3] Qinpeng Guo, Shanghong Zhao, Study on propagation characteristics of laser beam through the near space, Journal of Laser & Infrared 35 (2) (2008) 6–10.
[4] A.V. Push, Predication of thermal displacement in spindle units, Journal of Soviet Engineering Research. 5 (5) (1995) 57–62.
[5] Yao Lei, Study on the environmental flexibility technology of optical-terminal-equipment on near-space platform [D], vol. 3, Changchun University of Science and Technology, Changchun, 2010.
[6] Dezhi Sun, Research on the dynamic and static performances of mainshaft bearing test bench for aircrafts:[D], vol. 6, Herbin Industry University, Heilongjiang, 2006.
[7] A.K. Noor, Global–local methodologies and their application to nonlinear analysis, Finite Elements in Analysis and Design 2 (4) (1996) 333–346.
[8] A. GuPta, C.L. Chan, A. Chandra, BEM formulation for steady-state conduction-convention problems with variable velocities, Numerical Heat Transfer Part B Fundamentals 25 (4) (1994).
[9] C.C. Wong, S. Graham, Investigating the thermal response of a micro-optical shutter, IEEE Transactions on Components and Packaging Technologies (2003) 26–37.
[10] Gabriela Huminic, Angel Huminic, Heat transfer characteristics of a two-phase closed thermosyphons using nanofluid, Experimental Thermal and Fluid Science 35 (2011) 550–557.
[11] Dong Yang, Jie Pan, Chenn Q. Zhou, Xiaojing Zhu, Qincheng Bi, Tingkuan Chen, Experimental investigation on heat transfer and frictional characteristics of vertical upward rifled tube in supercritical CFB boiler, Experimental Thermal and Fluid Science 35 (2011) 291–300.
[12] Yulun Qiu, Effect of the space environment on optical remote sensor, Journal of Environmental Technology 43 (2005) 45–50.